Test in magnetic field of a drift chamber operated with a helium based gas mixture.

C.Avanzini,G.Ciapetti,E.De Lucia,F.Lacava,C.Luisi
G.Margutti,A.Nisati,M.Passaseo,L.Pontecorvo,S.Rosati
S.Veneziano,M.Verzocchi
Dipartimento di Fisica Università "La Sapienza" and
Sezione INFN - Roma - Italy
P.Valente
Dipartimento di Fisica Università "Tor Vergata" and
Sezione INFN Roma II - Italy
C.Bacci,F.Ceradini
Dipartimento di Fisica Università "RomaTre" and
Sezione INFN Roma III - Italy
G.Bencivenni,A.Calcaterra,R.de Sangro,P.De Simone
G.Felici,G.Finocchiaro,M.Piccolo
Laboratori Nazionali di Frascati dell'INFN - Frascati - Italy

Abstract

We report on a beam test of a small prototype of the KLOE drift chamber in magnetic field. The chamber was operated with a 90% He - 10% iC_4H_{10} gas mixture. Drift space-time relations were studied. The average spatial resolution is about 110 μm in absence of magnetic field and 120 μm in a 0.6 T magnetic field. Measurements of the primary ionization and drift velocity are reported. The measurement of dE/dx in a He-based gas mixture is also discussed.

1 Introduction

The KLOE experiment at the e^+e^- $\phi-$factory DAΦNE of the Laboratori Nazionali di Frascati is optimised to study the CP-symmetry violation in the decays of neutral kaons. The main goal of the experiment is the measurement of the ratio ϵ'/ϵ with a precision of $O(10^{-4})$ [1].

The tracking detector of the experiment is a cylindrical drift chamber [2], with a diameter of 4.0 m and a length of 3.4 m, surrounded by a hermetic calorimeter, both immersed in a 0.6 T axial magnetic field. The long decay path of the K_L ($\lambda_L = 3.5$ m) and the isotropic distribution of the charged decay products have suggested for this detector a continuous and uniform filling of the sensitive volume with stereo cells. The chamber is made of 58 concentric rings of drift cells oriented with alternated stereo angles. The drift cells (12582 in total) are almost square in shape with a ratio of field to sense wires $3:1$. The first 12 rings have cells of area $2 \times 2\pi/3$ cm^2, while the 46 outer rings of area $3 \times \pi$ cm^2.

The whole design of the chamber and the choice of materials [3] is intended to minimize the effect of multiple scattering, the conversion of photons and the K_L regeneration: the inner and outer cylindrical walls and the end plates are in carbon fiber, the field wires are in aluminum and a very light He-based gas mixture has been chosen. Results of several tests done on small size prototypes to study the structure and dimensions of the drift cell have been reported [2]. A full-length wedge of the chamber [4] has been built and tested on a beam to study the all-stereo drift cell configuration.

All previous measurements on prototypes were done without magnetic field. We present the results of a test of a small-size prototype with field varying from 0 to 0.9 T. The test was done with a 50 GeV/c pion beam. Beam particles traversing the prototype were measured with a precise external tracking system.

2 The prototype of the KLOE chamber

The prototype consists of 49 drift cells, arranged in seven layers of seven cells as shown in fig.1. They have an almost square shape of $3 \times \pi$ cm^2 and reproduce a section of the KLOE drift chamber at the centre in the longitudinal direction. No stereo angle was implemented in this prototype. The wires are 55 cm long: 25 μm diameter gold-plated tungsten sense wires and 80 μm diameter silver-plated aluminum field wires, as used in the construction of the real detector [3].

The end-plates and the walls of the prototype were machined in aluminum and the sense wires were positioned with feedthroughs on the end-plates with an accuracy of about 20 μm. The high voltage was supplied to the sense wires by seven printed boards at one end-plate while three printed boards, each with 10 preamplifiers were connected to the other end-plate. Only 30 cells, the 5 central cells on 6 layers numbered in fig.1, were read out.

The preamplifiers were the ones chosen for the KLOE drift chamber, Tektronics VTX [5] with a gain of 1 mV/fC on a 50 Ω load. Each preamplifier was followed by a $\times 3$ voltage amplifier with two outputs. One output was discriminated and sent to a TDC with 1 ns LSB. The discriminator threshold was set at 12 mV to detect the first arriving electron (the average single cluster pulse height was 35 mV at 1900 V). The second output was used to measure the charge with a 0.25 pC LSB charge integrating ADC with a 4 μs time gate.

A gas mixture $90\%He - 10\%iC_4H_{10}$ was supplied by mass flowmeters at a rate of about 10 l/h. During the test the temperature was between 19.1 and 20.9 ^{0}C and the atmospheric pressure between 950 and 972 mbar.

3 Precision trackers

Two identical reference trackers [6] were fixed to the side walls of the prototype (fig.2) to precisely track the beam particles traversing the prototype. Each tracker consists of 26 Al tubes, 3.050 cm diameter and 500 μm thickness, arranged in three layers (9+8+9 tubes) with the central layer offset by one tube radius and a distance of 4 cm between the layers. These tubes, with a 100 μm thick Cu-Be wire, were operated in limited streamer mode with a gas mixture $40\%Ar - 60\%iC_4H_{10}$ at 5.7 kV. The frames supporting the tubes were machined with an accuracy of 30 μm. The large signals (>200 mV) were discriminated with a threshold of 15 mV and were read-out by a 125 ps LSB TDC. The tubes were parallel to the drift cells of the prototype.

The prototype and the two reference trackers were rigidly connected together to assure the stability of the relative position of the wires.

4 Experimental layout and data acquisition

The test was performed at the X7 beam in the CERN West Area, where a large magnet was available. The useful magnet aperture was 80×62 cm^2 transverse to the beam, and 3.70 m along the beam direction. The prototype with the two reference trackers were positioned in the middle with the wires normal to the beam and parallel to the field direction. Additional tracking devices were placed upstream and downstream. Two MWPC's (10×10 cm^2) with delay line read-out, capable of 300 μm resolution, were used to track the beam particles both vertically and horizontally. The trigger was formed by the coincidence of two fast scintillation counters of 10×10 cm^2 area. The beam in the chamber had a vertical spread with σ=1.5 cm; several samples of 50 and 100 thousands of events were collected to get a uniform illumination over the cells.

The data acquisition was done with an embedded OS9 system based on VME 68030 CPU and a VAX-Station. The data from the TDC's and the ADC's were read out by the CPU and recorded on Exabyte cassettes. A data spying process running on the workstation used a fraction of events to generate histograms for monitoring and for event display. The average acquisition rate was 180 events per burst.

The data were collected with a 50 GeV/c π^+ beam with a small contamination of positrons. About 2.5 millions of events were recorded at 1850 and 1900 V and for different values of the magnetic field, B = $(0 - 0.9)$ T. A detailed list of the data sample is given in Table 1.

5 Drift space-time relation

Before studying the prototype, we have derived the drift space-time relations for the tubes of the reference trackers. This was done by an iterative procedure [7] starting from a simple first approximation $r - t$ relation and then deriving, by succesive iterations, a second order relation for the groups of four adjacent tubes illuminated by the beam. At the end of this calibration procedure the residuals were 50-100 μm and the single wire resolution was about 75 μm. The calibration procedure was repeated for each value of the magnetic field thus taking into account the effect of changes of the drift velocity and Lorentz angle in the tubes. A check of the calibration is the measurement of the bending angle between the centres of the reference trackers placed 53 cm apart: 1.84 ± 0.03 mrad at 0.6 T and 2.75 ± 0.02 mrad at 0.9 T, to be compared with the nominal values of 1.91 and 2.86 mrad respectively.

The drift space-time distributions for the cells of the prototype were then derived from the drift times and the distance of closest approach to the wire of the track reconstructed in the reference trackers. An example for one cell at 1900 V and B = 0 T is reported in fig.3. These distributions appear roughly parabolic on either side of the wire with some deviations close to the wire and at the cell border. In order to parametrize the $r - t$ relations, we have averaged the distributions over intervals of 300 μm of the distance from the wire. The averaged distributions for one cell at 1900 V and for B = 0, B = 0.6, B = 0.9 T are presented in fig.4. The effect of the magnetic field is evident.

We have parametrized the $r - t$ relation with the function

$$t = N \cdot atan(a \cdot r^2 + b \cdot r)$$

that is more effective than a parabola in the regions at the borders of the cell. An example for B=0.6 T is reported in fig.5.
The residuals of the distance reconstructed with the $r - t$ relation and the distance of closest approach extrapolated from the reference trackers, are smaller than 100 μm over most of the cell. Two examples are shown in fig.6.

The width of the residuals, that is locally independent of the $r - t$ parametrization, is the convolution of the spatial resolution of the chamber and of the extrapolation error of the reference trackers (30 μm - see below). At 1900 V the resolution in the center of the drift space is about 110 μm for B = 0 T (fig.7a) and 120 μm for B = 0.6 T (fig.7b). The larger resolution that we observe with magnetic field is justified in the following section.

6 Effect of the magnetic field

The magnetic field modifies the value and the direction of the drift velocity. These two effects are summarized by the Lorentz angle α_L in the Tonks' scaling law [8]:

$$v(B, E) = v(B = 0, E = E cos\alpha_L).$$

The validity of this scaling law is assumed in most calculations based on the transport equation, though some deviations have been observed [9]. Since it is difficult to determine the values of the Lorentz angle in the radial electric field of our cells, we studied the effect of the magnetic field by comparing the experimental results with the predictions by GARFIELD [10] and MAGBOLTZ [11] programs. The $r - t$ relations from the data and from the calculations are shown in fig.8, for one cell at 1900 V when B=0. and 0.6 T, and are in good agreement. The difference between the drift distances at B = 0 and B = 0.6 T, at a given drift time, observed in our data is compared with the results of the calculations in fig.9 and with the best resolution in our cells. The effect of the magnetic field on the $r-t$ relation exceeds the resolution for drift times larger than 200 ns (about 0.5 cm in drift space from the wire). These results show good agreement between the measurements and the calculations for the used $He - iC_4H_{10}$ mixture and make us confident in the use of the calculations with the actual stereo geometry.

7 Fit of the spatial resolution

In order to measure some of the parameters which characterize the gas mixture, we have studied the spatial resolution as a function of the drift distance [12]. The contributions to the spatial resolution are due to: i) primary ionization statistics σ_I, ii) electron diffusion in the gas σ_D, iii) electronics σ_{el}, iv) extrapolation of the track reconstructed by the external trackers σ_{extr}. Adding in quadrature all these effects we fit the data with the following function:

$$\sigma_{tot}^2 = \sigma_I^2 + \sigma_D^2 + \sigma_{el}^2 + \sigma_{extr}^2$$

fig.10 shows a fit of the spatial resolution in one cell at 1900V.
The contribution of the primary ionization is:

$$\sigma_I^2 = \frac{\lambda^2}{2} + R^2 - \bar{l}^2$$

where λ is the mean free path between two ionizing acts, R is the distance of closest approach of the ionizing particle to the wire and $\bar{l}$ is the mean distance from the wire of the point where the cluster has been produced. We find $\lambda = (590 \pm 10)$ μm corresponding to a value of the primary ionization $n_p = \lambda^{-1} = (16.9 \pm 0.3)$ cm^{-1} for 50 GeV/c pions. When this result is scaled to the energy loss of a minimum ionizing particle we obtain $n_p = (12.3 \pm 0.2)$ cm^{-1}. This number can be compared with previous measurements and with predictions based on transport equations: (13 ± 2) cm^{-1} measured with the first prototype of the KLOE drift chamber [13], (12.5 ± 0.5) cm^{-1} measured with 200 MeV/c pions [14], and finally 12.7 cm^{-1} computed by Sharma and Sauli [15].

An alternative determination of the primary ionization can be derived from the time distribution of the first electron arriving to the sense wire as a function of the drift distance. Convoluting the distribution of the distance from the wire of the primary clusters, l, with the other mentioned contributions, we have fitted the measured time distribution obtaining for the primary ionization $n_p = (15 \pm 1)$ cm^{-1} [12] consistent with the value reported above.

The contribution of σ_D due to the electron diffusion in the gas has been parametrized as the product of a term depending on the number n of ionized electrons, out of the total, concurring to the arrival of the first electron to the sense wire [16] times the ratio of the diffusion coefficient $D(E)$ and the drift velocity $w(E)$ of the electrons in the gas

$$\sigma_D^2 = \frac{1.64}{2 \ln n} \cdot \frac{2D(E)}{w(E)} \cdot R$$

Simulating the diffusion with MAGBOLTZ we have observed that the ratio $D(E)/w(E)$ is almost constant in the interval $R = 0.2 - 1.0$ cm, both for B = 0 and B = 0.6 T.
The best fit to the resolution gives the following results:

$$n = (11 \pm 3)$$

$$\left(\frac{2 \cdot D}{w}\right)_{B=0} = (3.0 \pm 0.2)\, 10^{-4} cm$$

$$\left(\frac{2 \cdot D}{w}\right)_{B=0.6} = (4.4 \pm 0.4)\, 10^{-4} cm$$

corresponding to $\sigma_D \sim 100$ μm for B = 0 and $\sigma_D \sim 120$ μm for B = 0.6 T at a distance of $R = 1$ cm, consistent with the values calculated in ref.[15] at B

= 0 T. The larger value of σ_D at B = 0.6 T justifies the deterioration of the resolution in presence of magnetic field reported in section 6.
Electronics, due to the time jitter of the trigger and of the discriminated signal from the wire, gives to the resolution a constant contribution, σ_t, in the time domain. From the fit to the spatial resolution, with $\sigma_{el} = w(R) \cdot \sigma_t$, we derive $\sigma_t = (2.9 \pm 0.3)$ ns.

For the last contribution, the track extrapolation, we derive $\sigma_{extr} = (27 \pm 3)$ μm, consistent with the error of the track position measured with 6 tubes of the reference trackers, each with a resolution of 75 μm.

8 Drift velocity

The unsaturated drift velocity in helium-isobuthane mixtures and the almost radial electric field determine in our cells a rapidly increasing drift velocity for electrons approaching the wire. The drift velocity as a function of the distance from the wire is derived by a local fit to the $r - t$ distribution. Our results as a function of the local electric field in the cell (calculated with the GARFIELD program) are shown in fig.11 and compared with previous dedicated measurements [17], [18] and with calculations [15]. All data are in good agreement: minimal deviations could be justified in terms of small changes in the operating conditions (pressure, gas mixture) for the different measurements .

9 Drift cell efficiency

The cell efficiency as a function of the applied voltage was determined using a small set of data (10^4 events per voltage value) collected at the beginning of the data taking. This efficiency, defined as the ratio of the number of points measured in the cell with a distance < 500 μm from the track reconstructed by the precision trackers and the total number of tracks reconstructed and crossing the cell, is higher than 0.996 for high voltage values > 1850 V (fig.12).

The efficiency as a function of the distance from the wire is evaluated as the ratio between the number of particles with a distance of less than 5 σ from the track reconstructed by the reference trackers, and the number of tracks in the reference trackers. The efficiency for one cell at 1900 V is shown in fig.13 as a function of the distance from the wire. The loss of efficiency close to the wire and at the border of the cell is due to the worse accuracy of the $r-t$ parametrizations in these regions of the cell.

10 dE/dx measurement

For the measurement of the energy loss, we have analysed only the data at 1850 V for two reasons: at 1900 V the ADC data were some times overflowed and at 1850 V we collected a larger amount of data (see Table 1). Anyway a lower voltage can only affect the time resolution based on the arrival of the first cluster not the collection of the total charge. A typical charge distribution is shown in fig.14. The ratio of the full width at half maximum of the distribution to the peak value is about 60% for a single cell.

We define "hit" a cell whose ADC signal after pedestal subtraction exceeds three times the pedestal width, and we select events with at least 4 hits, a drift time less than 2.5 μs and an impact parameter less than 1.5 cm. The most probable value of the charge distribution, after equalization of the cells response, is 136 pC at 1850 V corresponding to a gas gain of (6.9 ± 0.7) 10^4 [19]. We have studied the behaviour of the gas amplification as a function of the voltage applied to the wire. We have verified that the most probable value of the charge follows exponentially the variation of the high voltage and that the charge collected is constant up to a distance of 1.4 cm from the wire (fig.15). We thus conclude that there are no space charge effects neither gas gain saturation in the chosen working conditions.

The dE/dx resolution was measured using the truncated mean technique, combining several 5-hits events to simulate arbitrarily long tracks [20]. We observe that accepting the 80% lowest dE/dx values of the hits in the track we obtain the best resolution and we correctly reproduce the most probable value of the single cell charge distribution. For higher values of the accepted fraction, the resolution gets worse due to the inclusion of hits in the Landau distribution tail, while for smaller values the effect is related to the loss in statistics. The small fraction of rejected hits, as compared to argon-based mixtures, is due to the reduced Landau distribution tail in light gas mixtures. The effect is clearly visible even with only 10 hits (fig.17): the shape of the distribution of the lowest 8 hits is almost symmetric. The dE/dx resolution function is usually parametrized [21] as:

$$\sigma_{dE/dx} \propto N^a \cdot x^b$$

with N the number of samples and x their length (fig.16). In our gas mixture we measure $a = -0.49 \pm 0.01$, very close to the Poisson-law limit, and $b = -0.40 \pm 0.01$. The values measured for argon are: $a = -0.46$ and $b = -0.32$ [21].

In Table 2 several dE/dx resolutions measured with argon and helium based gas mixtures are listed. Comparing the different $\sigma_{dE/dx}$, evaluated with the above scaling law for $N = 100$ and $x = 1$ cm, we conclude that our gas mixture is competitive in energy loss measurements with the traditional argon and other helium mixtures.

Using 100 hits as a reference, with 50 GeV/c pions and 80% of accepted fraction, we measure a dE/dx resolution of $(4.2 \pm 0.1)\%$.

11 Conclusions

We have tested a drift chamber operated with a 90% helium−10% isobuthane mixture in magnetic field. The size and shape of the drift cells reproduce a small section of the KLOE drift chamber. A spatial resolution of 110 μm is measured over most of the cell; a small deterioration is observed in magnetic field and it is interpreted as due to diffusion. Measurements of the drift velocity as a function of the electric field, of the specific primary ionization and of the energy loss are reported. We show that, in spite of the small number of primary ion pairs compared with argon mixtures, the truncated mean technique provides a good dE/dx resolution for particle identification even in light helium based gas mixtures.

Acknowledgements

We are very grateful to our colleagues of the KLOE Chamber Group for encouraging the present test. It is a pleasure to mention here the kind help of Giles Barr, Lau Gatignon and J.Spangaard in organizing this test at CERN. We have to acknowledge the technicians who contributed to the construction of the detectors : M.Iannone, F.Pellegrino, G.Capradossi and M.Siteni for preparing the chamber; A.Di Virgilio, L.Iannotti for the precision trackers; S. DiMarco, F.Pulcinella and A.Rossi for the electronics.

HV	B = 0 T	B = 0.3 T	B = 0.6 T	B = 0.9 T
1850 V	900 K events		800 K events	
1900 V	400 K events	25 K events	400 K events	100 K events

Table 1: Statistics of the event samples

Mixture	$\sigma_{dE/dx}$ $x = 1$ cm, $N = 100$	Comments
$80\% Ar - 20\% CH_4$ [22]	5.8%	10 atm, 80 cm, 200 samples 70% accepted,$\sigma_{meas} = 2.7\%$
$80\% He - 20\% iC_4H_{10}$ [23]	4.6%	1 atm, 5.6 cm, 7 samples 60% accepted,$\sigma_{meas} = 18.7\%$
$50\% He - 50\% iC_2H_6$ [24]	4.2%	1 atm, 18 cm, 10 samples 80% accepted,$\sigma_{meas} = 10.1\%$
$80\% He - 20\% iC_4H_{10}$ [25]	4.9%	1 atm, 70 cm, 35 samples 60% accepted,$\sigma_{meas} = 6.2\%$
$90\% He - 10\% iC_4H_{10}$ [4]	4.5%	1 atm, 30 cm, 10 samples 80% accepted,$\sigma_{meas} = 9.3\%$
$90\% He - 10\% iC_4H_{10}$ [26]	4.6%	1 atm, 48 cm, 16 samples 68% accepted,$\sigma_{meas} = 8.4\%$
$90\% He - 10\% iC_4H_{10}$	4.2%	1 atm, 300 cm, 100 samples 80% accepted,$\sigma_{meas} = 4.2\%$

Table 2: Comparison of some dE/dx measurements in drift chambers with the resolution extrapolated from the present test (last row).

References

[1] The KLOE Collaboration: "The KLOE Detector Technical Proposal", LNF-93/2 (1993).

[2] The KLOE Collaboration: "The KLOE Central Drift Chamber", Addendum to the KLOE Technical Proposal, LNF-94/028 (IR), (1994)

[3] G.Bencivenni et al.,The KLOE drift chamber construction,Nucl. Instr. and Methods in Physics Research A419 (1998) 320.

[4] A.Andryakov et al., Nucl. Instr. and Methods in Physics Research A404 (1998) 248.

[5] R.J.Yarema et al.,IEEE Trans.Nucl.Sci. 39 (4) (1992) 742.

[6] C.Avanzini et al., Nucl. Instr. and Methods in Physics Research A367 (1995) 154,

[7] C.Avanzini et al.,Local autocalibration of drift tubes, KLOE Note n.141, March 1995, Internal Note INFN/Università di Roma N.1062.
A. Calcaterra, R. De Sangro, G. Finocchiaro,High precision limited streamer drift tubes, KLOE note n.127 Dicember 1994.

[8] W. Blum and L. Rolandi,Particle Detection with Drift Chambers, Springer-Verlag (1993).

[9] T.Kunst et al.,Nucl. Instr. and Methods in Physics Research, A324 (1993) 127.

[10] R.Veenhof,Garfield,A drift chamber simulation program, CERN Program Library, W5050.

[11] S.F.Biagi, Nucl. Instr. and Methods in Physics Research, A283 (1989) 716.

[12] C.Luisi,"Study of the microscopic parameters of the KLOE helium based gas mixture in prototypes", KLOE memo n.78, December 1996, and thesis at the University 'La Sapienza' - Roma (1996), unpublished.

[13] G.Bencivenni et al., "The prototype 0 of the KLOE tracking chamber", KLOE note n.79-93

[14] G.Cataldi et al.,Nucl. Instr. and Methods in Physics Research A386 (1997) 458.

[15] A.Sharma and F.Sauli, Nucl. Instr. and Methods in Physics Research A350 (1994) 470.

[16] V.Palladino and B.Saudoulet, Nucl. Instr. and Methods 128 (1975) 323.

[17] P.Bernardini et al., Nucl. Instr. and Methods in Physics Research A355 (1995) 428.

[18] C.Grab,ETHZ IMP PR 92-5.

[19] E. De Lucia,"Misure di ionizzazione specifica in prototipi della camera a deriva dell'esperimento KLOE",thesis at the University 'La Sapienza' - Roma (1996),unpublished.

[20] G.Finocchiaro, M.Piccolo, P.Valente,"dE/dx resolution in a He-Iso 90:10 gas mixture with 50 GeV/c pions", KLOE Memo n.33, October 1995.

[21] W.Allison and J.H.Cobb, Ann. Rev. Nucl. Part. Sci. 30 (1980) 253.

[22] D.Fancher et al., Nucl. Instr. and Methods in Physics Research 161 (1979) 383.

[23] I.A.Yadigaroglu et al., Nucl. Instr. and Methods in Physics Research A323 (1992) 322.

[24] M.Aoki et al., Nucl. Instr. and Methods in Physics Research A330 (1993) 55.

[25] K.K.Gan et al., Nucl. Instr. and Methods in Physics Research A374 (1996) 27.

[26] E.Borsato et al.,Study of ionization losses in He-based gas mixtures", to be published in Nucl. Instr. and Methods in Physics Research A.

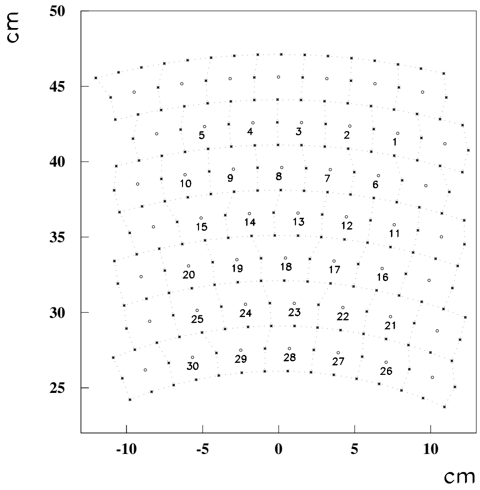

Figure 1: Layout of the drift cells in the prototype

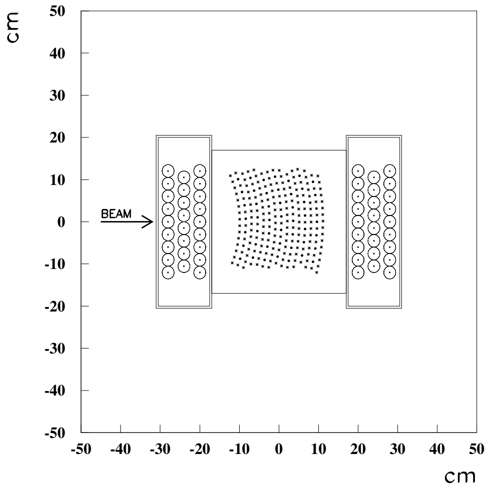

Figure 2: View of the prototype with the reference trackers

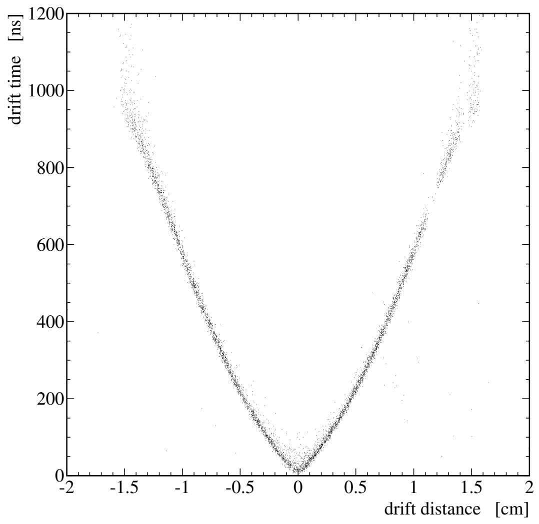

Figure 3: Drift space-time distribution for B = 0 T

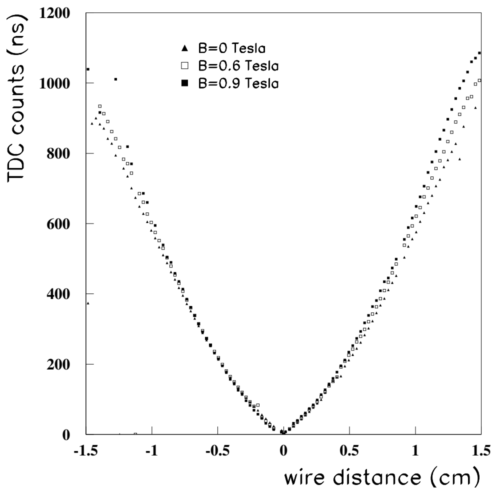

Figure 4: Average drift space-time distributions for different values of the magnetic field

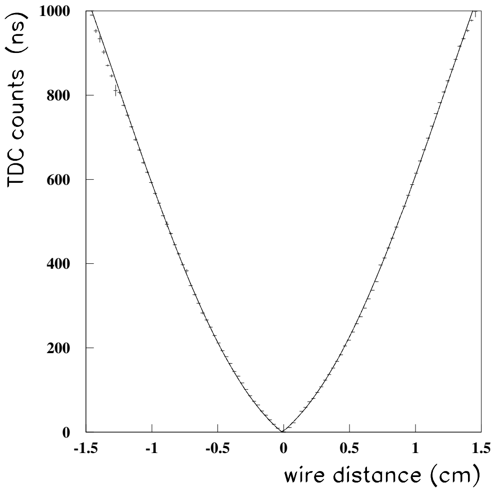

Figure 5: Example of the arctangent parametrization for B=0.6 T

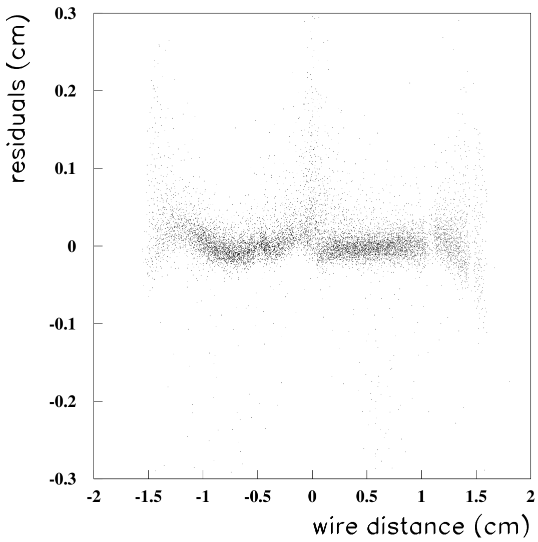

a

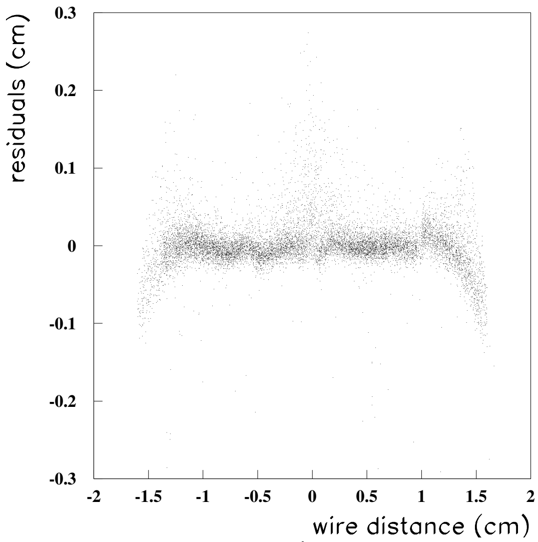

b

Figure 6: Residuals for the arctangent parametrization for B = 0 T (a) and for B = 0.6 T (b)

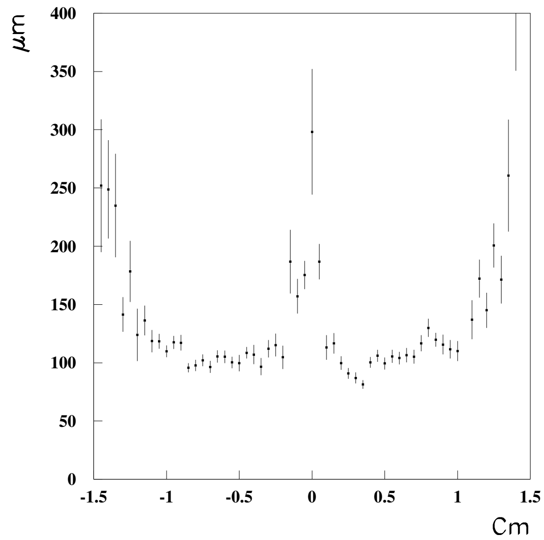

a

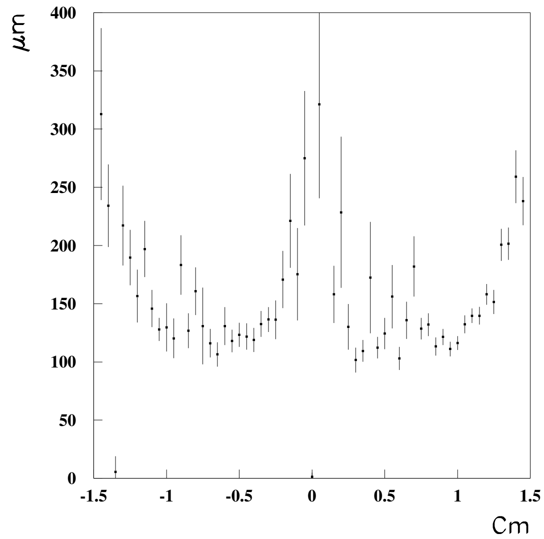

b

Figure 7: Resolution as a function of the distance from the wire for B = 0 T (a) and for B = 0.6 T (b)

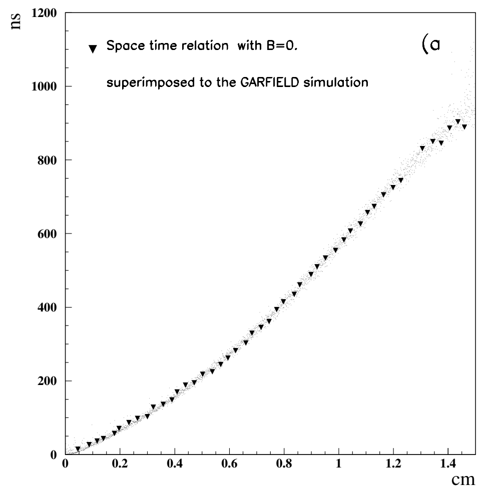

a

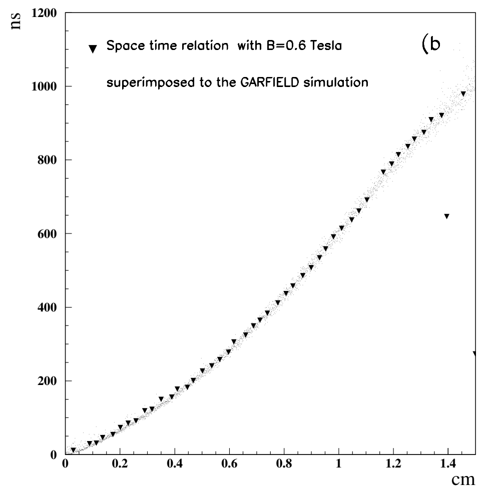

b

Figure 8: Drift space-time experimental distributions with superimposed Garfield predictions for B=0. T (a) and B=0.6 T (b)

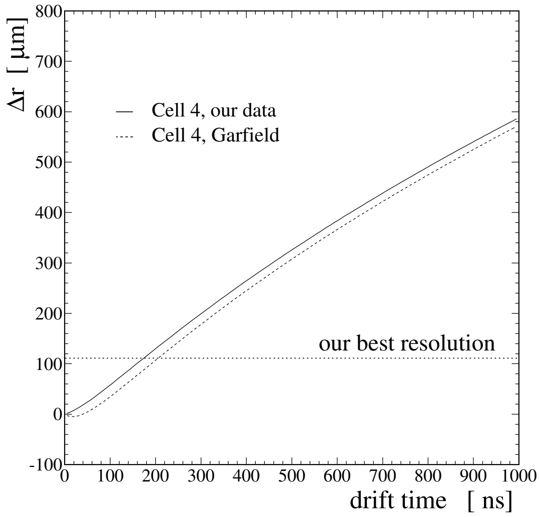

Figure 9: Difference between the drift distances without and with magnetic field (B = 0.6 T), as a function of the drift time, from data and Garfield.

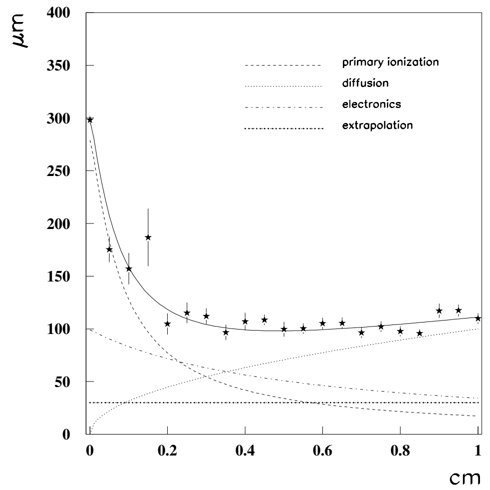

Figure 10: Fit of the different contributions to the spatial resolution versus the drift distance.

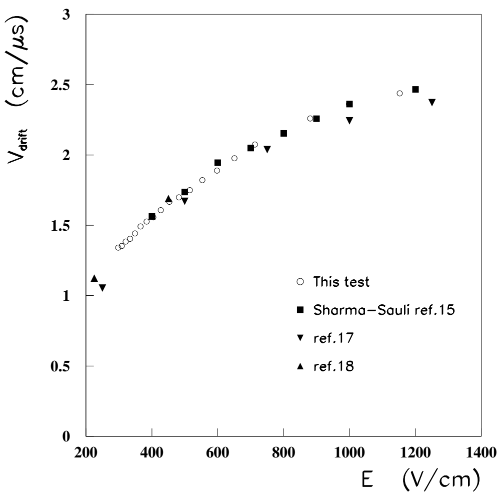

Figure 11: Drift velocity as a function of the electric field

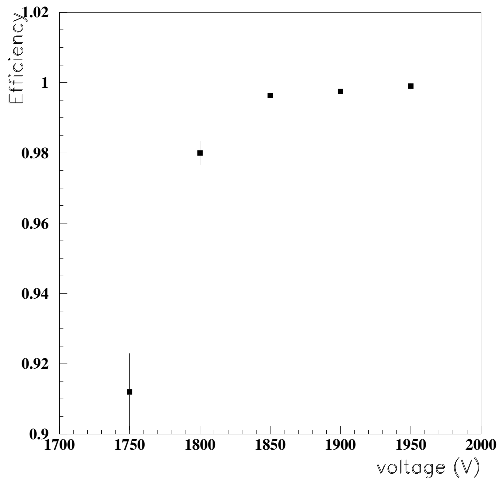

Figure 12: Efficiency as a function of the applied voltage

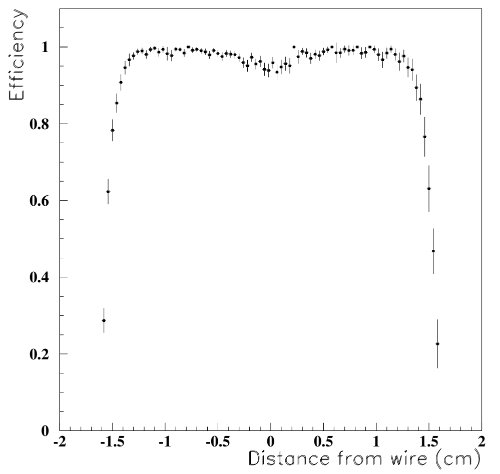

Figure 13: Efficiency as a function of the distance from the sense wire at 1900 V.

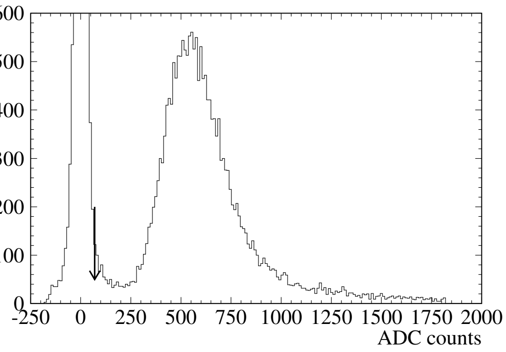

Figure 14: A typical ADC spectrum; the arrow shows the 3σ cut

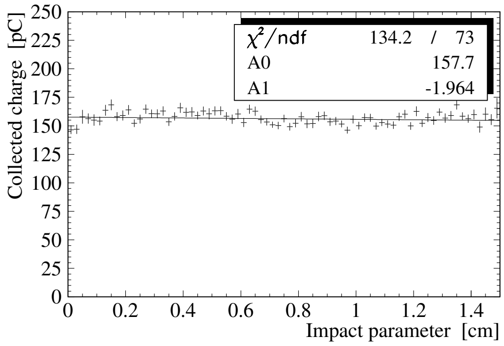

Figure 15: Collected charge as a function of the impact parameter

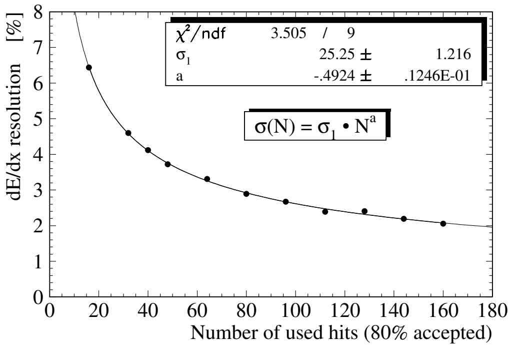

Figure 16: dE/dx resolution vs number of used hits.

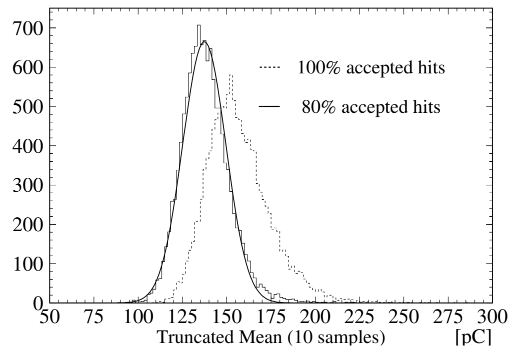

Figure 17: Effect of the truncation in samples of 10 hits.